Volume 7, No. 5 May, 2026
p ISSN 2723-6927-e ISSN 2723-4339

Analysis of Variations Apparent Diffusion Coefficient (ADC) Values in Brain Areas Using Dwi Resolve Sequence

Chankrisna Anggarayuda, Hernastiti Sedya Utami*, Kusnanto Mukti Wibowo, Pradana Nur Oviyanti, Fathur Rahman Nugraha
Universitas Muhammadiyah Purwokerto, Indonesia
Email: channkrisnna02@gmail.com, hernastitisedyautami@ump.ac.id*

Abstract
Magnetic Resonance Imaging (MRI) with Diffusion-Weighted Imaging (DWI) evaluates the microstructure of brain tissue through the Apparent Diffusion Coefficient (ADC) parameter. Although often used clinically, the accurate standardization of physiological values of ADCs is still a challenge due to the high regional variability. This study aims to analyze the difference in ADC values in various anatomical structures of the adult brain using the DWI Readout Segmentation of Long Variable Echo-trains (RESOLVE) sequence. This retrospective analytical observational study involved 12 normal subjects examined using 1.5 Tesla MRI. Measurements were made manually on 14 anatomical structures using a circular Region of Interest (ROI) (±20 mm²). Reliability is validated by the Intraclass Correlation Coefficient (ICC). Statistical analysis included Repeated Measures ANOVA, Spearman correlation (age), and Wilcoxon test (grey vs White matter). The results showed that the ROI had excellent reliability (ICC 0.845–0.998). There was a very significant difference in ADC values between anatomical structures ($p < 0.001$; Partial $\eta^2 = 0.700$), with an average range of 0.70–0.83 $\times 10^{-3}$ mm²/s. There was no significant correlation between age (22–68 years) and regional ADC fluctuations ($p > 0.05$). However, the ADC of Grey matter was found to be significantly higher than that of White matter ($p = 0.002$). In conclusion, the RESOLVE DWI sequence results in reliable ADC measurements. Variations in diffusion values are inherently dependent on anatomical location and tissue type, but are very stable with age.
Keyword: magnetic resonance imaging; diffusion-weighted imaging; apparent diffusion coefficient; RESOLVE; Brain Tissue Structure

INTRODUCTION

Magnetic Resonance Imaging (MRI) is a non-invasive imaging modality that has advantages in the evaluation of soft tissues, especially the central nervous system, because it is able to provide high tissue contrast, good spatial resolution, and does not use ionizing radiation (Saltarelli et al., 2025; Squirting et al., 2024). The development of advanced sequencing in MRI allows the acquisition of tissue microstructural information in addition to conventional anatomical images (Martinez-Heras et al., 2021). One of the techniques that is widely used is Diffusion-Weighted Imaging (DWI), which is sensitive to the movement of water molecules and is affected by cell density as well as tissue integrity (Martinez-Heras et al., 2021; Palombo et al., 2025). From this technique, quantitative parameters are obtained Apparent Diffusion Coefficient (ADC), which represents the level of water diffusivity in brain tissue (Johansson et al., 2024; Spencer et al., 2025).

ADC values have been reported to have good reproducibility, both intra- and inter-scanner, and show consistency in MRI scanners with magnetic field strengths of 1.5 Tesla and 3 Tesla (Grech-Sollars et al., 2015; Merhemic et al., 2018). In clinical practice, ADC parameters are widely used in a variety of diagnostic contexts, including to determine non-infiltrative zones in medulloblastoma (Luo et al., 2022; Marupudi et al., 2016; Pehlivan et al., 2024), distinguish High-grade glioma and metastasis through ADC values of edema Expert (Caravan et al., 2018), as well as identifying Core infarction in acute ischemic stroke based on a specific threshold value (Lopez-Mejia & Roldan-Valadez, 2016). In addition, changes in ADC values were also reported to be related to the dynamics of cerebrospinal fluid in hydrocephalus conditions (Osawa) et al., 2021).

Although ADC is a widely used quantitative parameter, ADC values in brain tissue are not homogeneous. Variations in tissue microstructures, such as nerve fiber orientation and cell density, cause differences in ADC values between anatomical areas of the brain (Ghaderi et al., 2025; Johansson et al., 2024; Spencer et al., 2025). Studies on brain and fetal development show that ADC values are highly sensitive to microstructural changes during the maturation process (Calixtus et al., 2024; In Trani et al., 2019), as well as that structural disorders in pathological conditions such as Intrauterine growth restriction (IUGR) can significantly affect ADC values (Chandra Sekhar et al., 2024; Meijerink et al., 2025; Moradi et al., 2020). Although the context differs from that of the adult population, the findings indicate that the characteristics of the microstructure and tissue composition play an important role in determining the diffusion value of water. In the adult population, aging factors as well as changes in perivascular fluid dynamics have also been reported to affect the distribution of ADC values in brain tissue (Sotardi et al., 2021; Richmond et al., 2022). Therefore, an understanding of the regional variation of ADC values in the adult brain is important to support quantitative interpretation in radiology practice.

The accuracy of ADC value measurements is greatly influenced by the quality of the DWI sequence used. Conventional DWI based Single-shot echo-planar imaging (ss-EPI) has limitations in the form of geometric distortion, artifacts Susceptibility, as well as decreased image quality in areas adjacent to bone structures or sinuses, which could potentially affect the accuracy of ADC values (Okuchi et al., 2022; Palombo et al., 2025; Zhou et al., 2022). To overcome these limitations, a Readout Segmentation of Long Variable Echo-trains (RESOLVE), which is the Readout-segmented echo-planar imaging which is able to reduce geometric distortion and improve the spatial resolution of the image (Ahn et al., 2024; Okuchi et al., 2022). RESOLVE DWI sequences have been applied to a variety of neurological conditions, including stroke and brain tumors (Okuchi et al., 2022). However, studies that specifically evaluate variations in ADC values in different areas of brain anatomy using RESOLVE DWI sequencing are still limited in the literature.

This study aimed to analyze the variation in ADC values in several areas of the adult brain using RESOLVE Diffusion-Weighted Imaging (DWI) sequences. The analysis is focused on the comparison of ADC values between brain structures in the same individual, so that it is expected to provide an initial picture of the regional ADC value distribution pattern and support the use of quantitative MRI imaging in clinical practice. This research is expected to provide both theoretical and practical benefits. Theoretically, this study enriches the understanding of the quantitative parameters of diffusion MRI in normal adult brain tissue, provides baseline values of ADCs for various anatomical structures of the brain, as well as confirms the reliability of RESOLVE DWI sequences in producing accurate and reproducible ADC measurements. Practically, this study is useful for radiologists and clinicians as a baseline reference in the quantitative interpretation of DWI to identify abnormal diffusion patterns in pathological conditions such as stroke, brain tumors, and neurodegenerative diseases. For MRI technicians and medical physicists, this study provides technical insights on optimizing RESOLVE DWI sequences to minimize artifacts and improve image quality. For hospital radiology installations, these findings support consistent standardization of quantitative MRI protocols, and for subsequent academics and researchers, they serve as a foundation for further studies of ADC changes in specific neurological diseases or the expansion of analyses in larger populations.

RESEARCH METHOD

This research used a quantitative approach with an observational analytical design and a retrospective method. The research was carried out at the Radiology Installation of the Dadi Keluarga Purwokerto General Hospital in the period of December 2025 to January 2026. The research data was in the form of Magnetic Resonance Imaging (MRI) images of the brain in adult patients with clinical and radiological findings within normal limits. All examinations were performed using a 1.5 Tesla MRI system with a RESOLVE DWI sequence that produced an ADC map.

The sampling technique used the Total Sampling method on all retrospective data during the study period, which initially amounted to 40 patients. All of the data was then evaluated based on inclusion and exclusion criteria. Inclusion criteria included adult patients over 18 years of age who underwent a complete brain MRI examination with RESOLVE DWI sequence and ADC maps, and did not show intracranial structural abnormalities based on radiological reports. Meanwhile, exclusion criteria include the presence of significant image artifacts, findings of focal lesions such as infarction, mass, demyelination abnormalities, and a history of neurological diseases that have the potential to affect the diffusion characteristics of brain tissue. Based on the evaluation of these criteria, as many as 28 subjects were excluded. In the end, 12 subjects (age range 22–68 years) were obtained whose images were clean of artifacts. The 12 image data were then validated directly by the Radiologist to ensure that the subject's brain anatomy was completely normal and clinically healthy, so that it was suitable for use as a final sample of the study.

Image analysis was carried out using MicroDicom Viewer software. The identification and determination of anatomical structures is validated by a radiologist to ensure the accuracy of the determination of ROI and anatomical suitability. In each subject, an ADC map obtained from the RESOLVE DWI sequence was analyzed. ROI is placed manually on 14 anatomical structures of the brain, namely frontal, anterior cranial base, parietal, brainstem, cerebellum, occipital, temporal, pons, centrum semiovale, basal ganglia, thalamus, vermis, substantia alba, and hippocampus. The ROI is circular in shape with an area of about ±20 mm^2 placed in the most representative area. The selection of this size is based on the standard MRI diffusion literature to minimize the partial volume effect, so that the ROI edge limits do not overlap or be affected by signals from cerebrospinal fluid (CSF), blood vessels, and surrounding tissues, especially when evaluating narrow structures such as the basal ganglia and pons. If more than one slice meets the representative criteria for a structure, the ADC value used is the average of the slice. ADC values are recorded in mm^2/s and reported in $\times 10^{-3}$ mm^2/s scale.

To ensure the reliability of the data and avoid observational bias, measurements were taken twice by the same researcher (intra-observer) with an interval of five weeks for all anatomical structures. The results of both measurements were then validated using the Intraclass Correlation Coefficient (ICC) test to prove that the consistency and precision of the ROI placement carried out was very stable and reliable.

The ICC model used is Two-way mixed effects with the Absolute agreement type, because all measurements are carried out by one observer and focused on the absolute conformity between measurements. The interpretation of the ICC value followed general criteria, i.e. <0.50 indicates poor reliability, 0.50–0.75 moderate, 0.75–0.90 good, and >0.90 very good. The ICC test is performed before the main analysis to ensure that the variation in the ADC values obtained reflects biological variation, not measurement errors.

Statistical analysis is focused on evaluating the variation in ADC values between anatomical structures in the same subject (Within-subject design). Descriptive analysis was used to obtain the mean values and standard deviations of the ADC. Furthermore, the normality test of the distribution of data on each anatomical structure was evaluated using the Shapiro-Wilk test. The selection of this test was based on the small number of study samples (N = 12), where the Shapiro-Wilk test is highly recommended because it has a high level of sensitivity (Power) to test normality on sample sizes below 50 subjects (Mishra P, Pandey C, 2019). Differences in ADC values in 14 anatomical structures measured repeatedly in the same subject were analyzed using parametric tests Repeated Measures ANOVA. The sphegicity assumption is checked with the Mauchly test, and if it is not met, correction is applied Greenhouse–Geisser. The magnitude of the effect is reported using the Partial eta squared value (Partial η^2). Analysis of the relationship between age and ADC values was performed using the Spearman correlation test because some variables were not normally distributed. Meanwhile, the comparison of ADC values by network type (Grey matter and White matter) was analyzed using the Wilcoxon Signed-Rank test because the data were paired. All statistical analyses were carried out with a significance level of $p < 0.05$.

RESULTS AND DISCUSSION

Region of Interest (ROI) Placement

The measurement of the ADC value is done by manually placing the Region of Interest (ROI) on the ADC map. The ROI is circular in shape with a uniform size (±20 mm²) and is placed in the most representative area of each anatomical structure of the brain. ROI placement is carried out by avoiding the boundaries of cortex, blood vessels, and areas that have the potential to contain image artifacts to improve the consistency and reliability of measurements.

An example of ROI placement on cortical and subcortical structures is shown in **Figure 1** as a representation of the measurement procedure applied consistently across the subject and the anatomical structure analyzed.

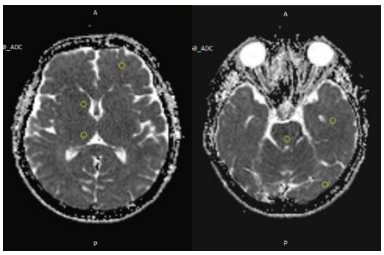

Figure 1. Example of ROI placement on cortical structures on ADC maps
Source: Research documentation, results of MRI image processing using MicroDicom Viewer (processed by researchers, 2026)

Statistical Analysis

Statistical analysis was conducted to evaluate differences in signal characteristics in 14 anatomical structures of the brain that were measured repeatedly in the same subject. The analysis stages include descriptive analysis, measurement reliability test, normality assumption test, ANOVA Repeated Measures parametric test with spherical correction, age correlation analysis, and comparison based on tissue type (Grey matter and White matter).

Descriptive Analysis

Descriptive analysis was performed to describe the distribution of mean values and variations of the data on each of the anatomical structures of the descriptive statistics presented on.

Table 1. Descriptive Statistics of ADC Values on Various Anatomical Structures of the Brain (N = 12)

Anatomical Structure	Red	Std. Deviation
Front	76344,67	2303,89
Previous Cranial Base	71856,33	7018,93
Parietal	82782,00	1654,29
Brainstem	75421,50	1721,24
Cerebellum	73918,00	2318,08
Occipital	82856,33	1733,11
Temporary	76656,17	2248,46
Pons	75646,33	1613,99
Centre Semioval	74904,25	1437,18
Basal Ganglia	74553,75	1773,00
Thalamus	76056,25	1845,65
Vermis	73459,75	1986,13
Substantia Alba	70405,42	3881,40
Hippocampus	83351,42	1905,07

Source: Primary data on ROI measurement results on MRI images (processed by researchers, 2026)

Descriptively, the highest average ADC values were found in the Parietal, Occipital, and Hippocampus (0.83), while the lowest values were found in the Substantia alba (0.70).

ICC Test

Before the main analysis, an intra-observer reliability test was carried out using the Intraclass Correlation Coefficient (ICC) with the Two-way mixed effects and Absolute agreement models to evaluate the consistency of ROI measurement.

Table 2. ICC Test Results

Region	ICC
Front	0,845
Previous Cranial Base	0,998
Parietal	0,992
Brainstem	0,993
Cerebellum	0,994
Occipital	0,991
Temporary	0,993
Pons	0,987
Centre Semioval	0,984
Basal Ganglia	0,991
Thalamus	0,991

Region	ICC
Vermis	0,993
Alba Substance	0,998
Hippocampus	0,994

Source: Test results processed by researchers, (2026)

The test results showed that the entire anatomical structure had an ICC value in the good to excellent category, with a value range between 0.845–0.998. Most structures show an ICC > 0.90, which indicates very high measurement reliability.

Normality Test

The normality of the distribution of ADC value data on 14 anatomical structures was analyzed using the Shapiro-Wilk test considering the limited sample size of the study (N = 12).

Table 3. Shapiro-Wilk Normality Test Results

Anatomical Structure	Statistic	df	Sig.(p)
Front	0,840	12	0,028
Previous Cranial Base	0,909	12	0,207
Parietal	0,940	12	0,496
Brainstem	0,946	12	0,583
Cerebellum	0,867	12	0,060
Occipital	0,969	12	0,904
Temporary	0,934	12	0,428
Pons	0,862	12	0,052
Centre Semioval	0,949	12	0,622
Basal Ganglia	0,965	12	0,853
Thalamus	0,968	12	0,893
Vermis	0,936	12	0,447
Substantia Alba	0,954	12	0,689
Hippocampus	0,970	12	0,908

Source: Test results processed by researchers, (2026)

The test results showed that most of the variables met the normality assumption (p > 0.05), with the exception of the frontal (p = 0.028). However, since only one variable does not meet the assumptions and the research design is repeated measures with a small sample size, parametric analysis can still be performed with the application of appropriate corrections to the ANOVA test.

Repeated Measueres Anova Test

The ANOVA Repeated Measures test was used to evaluate whether there was a statistically significant difference in ADC values between 14 anatomical brain structures measured repeatedly in the same subject. Since the data is normally distributed and comes from within-subject measurements, the Repeated Measures ANOVA parametric method was chosen. The results of the main analysis are presented in Table 3, while the test of Mauchly spericity assumptions is shown in Table 4.

Table 4. Repeated Measures ANOVA of ADC Values Across Brain Regions

Source	Df	F-value	p-value	Partial η²
ROI (Within-subject factor)	2,17	29,904	<0.001	0,700

Source: Test results processed by researchers, (2026)

ANOVA's Repeated Measures analysis shows significant differences between ROIs. The degree of freedom has been corrected using Greenhouse–Geisser because the assumption of sphegicity is not met. Partial value $\eta^2 = 0.700$ indicates a large effect size. These results answer the research question that each anatomical structure of the brain has distinctive and different characteristics of ADC values, which reflect the unique cellular composition and microstructure of each region. A Partial η^2 value of 0.700 indicates that about 70% of the variability of ADC values in this data can be explained by differences in anatomical structure types, rather than by variation between individuals.

Table 5. Mauchly's Test of Sphericity for ANOVA Repeated Measures Test

Effect	Mauchly's W	χ^2	df	p-value	Greenhouse–Geisser ε
ROI	<0.001	—	90	<0.001	0,209

Source: Test results processed by researchers, (2026)

The Mauchly test showed a violation of the sphericity assumption ($W < 0.001$; $p < 0.001$), so the ANOVA interpretation used a Greenhouse–Geisser correction ($\varepsilon = 0.209$). The Greenhouse–Geisser correction is applied because the assumption of sphericality is violated ($p < 0.001$; $\varepsilon = 0.209$), which means that the variance of the difference between the measurement pairs is not uniform. This correction functions to adjust the degree of freedom so that the resulting F and p-value remain accurate and do not produce false positives.

Table 6. Estimated Marginal Mean ADC Values by Brain Region

Region	Red	Std.Error	95% Lower Bound	95% Upper Bound
Front	76344,667	665,075	74880,847	77808,486
Anterior cranial base	71856,333	2026,191	67396,717	76315,950
Parietal	82782,000	477,552	81730,915	83833,085
Brainstem	75421,500	496,880	74327,875	76515,125
Cerebellum	73918,000	669,173	72445,161	75390,839
Occipital	82856,333	500,307	81755,165	83957,502
Temporary	76656,167	649,074	75227,565	78084,768
Pons	75646,333	465,918	74620,855	76671,812
Center semioval	74904,250	414,880	73991,106	75817,394
Basal ganglia	74553,750	511,821	73427,239	75680,261
Thalamus	76056,250	532,793	74883,580	77228,920
Vermis	73459,750	573,346	72197,825	74721,675
Substantia alba	70405,417	1120,465	67939,290	72871,543
Hippocampus	83351,417	549,946	82140,994	84561,840

Source: Results of analysis processed by researchers, (2026)

Table 6 shows the Estimated marginal Means ADC values of each brain region along with the standard error and 95% confidence interval obtained from the General Linear Model repeated measures model.

Analysis of Age Correlation and ADC Values

Spearman correlation analysis was performed to evaluate the relationship between the subject's age (22–68 years) and ADC values in each anatomical region separately. The results showed that there was no statistically significant correlation between age and ADC values across the anatomical regions ($p > 0.05$).

Table 7. Spearman Correlation Test Results between Age and ADC Values in Each Anatomical Region

No	Anatomy	Correlation Coefficient (ρ)	Value p (Sig. 2-tailed)	N
1	Front	0.389	0.212	12
2	Previous Cranial Base	-0.067	0.837	12
3	Parietal	0.067	0.837	12
4	Brainstem	-0.018	0.957	12
5	Cerebellum	-0.186	0.564	12
6	Occipital	0.221	0.491	12
7	Temporary	-0.172	0.594	12
8	Pons	-0.186	0.564	12
9	Centre Semioval	-0.479	0.115	12
10	Basal Ganglia	-0.165	0.609	12
11	Thalamus	0.095	0.770	12
12	Vermis	0.035	0.914	12
13	Substantia Alba	-0.179	0.579	12
14	Hippocampus	0.445	0.147	12

Source: Results of analysis processed by researchers, (2026)

The value of the correlation coefficient shows a weak and insignificant relationship, as shown in Table 7.

Comparison of Grey matter and White matter

To evaluate the difference in ADC values based on tissue type, anatomical structures were grouped into Grey matter and White matter. The average ADC value of each group is calculated for each subject.

Table 8. Wilcoxon Signed-Rank Test Results between Grey matter and White matter

Related-Samples Wilcoxon Signed Rank Test	
Total N	12
Test Statistic	.000
Standard error	12,748
Standardized Test Statistic	3,059
Asymptotic Sig. (2-sided test)	0,002

Source: Results of analysis processed by researchers, (2026)

The results of the Wilcoxon signed-rank test showed that there was a significant difference between the values of Grey matter and White matter ADCs ($Z = 3.059$; $p = 0.002$). The whole subject shows a consistent direction of difference.

Since $p < 0.05$, there is a significant difference between the ADC values of Grey matter and White matter.

This study aims to describe the variation in ADC values in various anatomical structures of normal adult brains using the RESOLVE DWI sequence. The descriptive analysis presented in Table 1 shows that each brain region has a different range as well as distribution of ADC values. These results show that the spread of ADC values in the normal brain is not homogeneous, but shows variations between anatomical regions.

Based on the results of measuring ADC values in normal adult brain areas using the RESOLVE DWI sequence, an average ADC value was obtained which showed variation between regions. The pattern of variation is in line with the microstructural characteristics of normal brain tissue that have been described in the MRI diffusion literature. The difference in ADC values in each region reflects the variation in composition Grey matter, White matter, as well as the orientation of nerve fibers that play a role in influencing the process of diffusion of water molecules (Johansson et al., 2024).

The distribution of mean ADC values across 14 anatomical structures of the brain showed a representative variation in the characteristics of the tissue microstructure, but remained within the normal physiological range corridor. The lowest average value was recorded in the substantia alba area of $70,405.42 \pm 3,881.40$ ($\approx 0.70 \times 10^{-3}$ mm²/s), while the hippocampus showed the highest average value of $83,351.42 \pm 1,905.07$ ($\approx 0.83 \times 10^{-3}$ mm²/s), which was followed by the occipital and parietal. The suitability of the reference value range in the entire anatomy also proves the reliability of the use of RESOLVE DWI sequences in producing accurate and precise baseline mapping according to the original conditions.

Analysis by network type shows a significant difference between Grey matter and White matter ($Z = 3.059$; $p = 0.002$). ADC value on Grey matter consistently higher than White matter on the whole subject. Physiologically, this is due to the Grey matter It contains more neural cell bodies and has a wider intercellular (extracellular) space. This condition allows water molecules to move more freely. Instead, the network White matter It is composed of dense nerve fibers tightly wrapped by a myelin sheath. Because the myelin sheath contains a lot of fat, this structure serves as a strong physical barrier in restricting the movement of water. It is this restriction of water molecule motion that ultimately makes the ADC value in the White matter become significantly lower (Helenius et al., 2002; Johansson et al., 2024). This difference also strengthens the suitability of the analysis results Repeated Measures ANOVA in this study.

The variability of ADC values reflected in the magnitude of standard deviations in several structures, especially in anterior cranial base (SD = 7,018.93) and alba substance (SD = 3,881.40) as shown in Table 1, indicates heterogeneity between study subjects. These variations may be influenced by several factors, including the subject's relatively wide age range (22–68 years), the existence of a partial volume effect, and limitations in determining ROI manually.

Analysis using the ANOVA Repeated Measures test showed that the difference in ADC values between regions was very significant (Partial $\eta^2 = 0.700$). These results confirm that variations in ADC values depend on specific anatomical regions and appear consistently in each subject. The analysis was not intended to show the biological superiority of one structure over

another, but rather to confirm the existence of physiological variations in the distribution of water diffusion in normal brain tissue.

Additional analysis of age factors using the Spearman correlation test showed that there was no significant association between age and ADC values in 14 anatomical regions evaluated ($p > 0.05$). The correlation coefficient is in the range of −0.479 in the semioval centrum to 0.445 in the hippocampus, and is entirely not statistically significant. These findings are in line with the basic theory of Hellenius et al. (2002), which reported that the average ADC score showed no significant difference by age on a normal brain DWI examination. Thus, the variation in ADC values found in this study purely reflects the regional characteristics of each anatomical structure rather than the influence of demographic factors. Likewise with research Sotardi et al. (2021) in fact, it shows a very significant change in ADC values during brain development in children aged 0–6 years, where ADC values progressively decrease along with the process of tissue maturation. This difference in findings can be logically explained by the difference in the subject population: this study used a sample of adult brains (22–68 years) that had completed the maturation process, so that the influence of age on the stability of ADC values was very minimal.

The use of RESOLVE DWI sequences provides technical advantages in the form of reduced geometric distortion and artifact susceptibility compared to conventional DWI, especially in areas adjacent to the cranial base and posterior structure of the fossa. The improved image quality allows for more accurate delineation of ROI (Figure 1), thus supporting the reliability of ADC value measurement and strengthening the interpretation of the regional distribution obtained.

Although this study provides a preliminary picture of the regional variation in ADC values in the normal adult brain, some limitations are noteworthy, especially the relatively small sample count ($N = 12$) and the manual use of ROI. Therefore, further research is recommended to involve a larger number of subjects, using a voxel-based approach, as well as evaluating the reliability between observers to improve the validity and generalization of the findings.

This research has several limitations. First, the sample size was relatively small ($N = 12$) due to the large number of subjects excluded to obtain normal brain criteria, thus limiting the generalization of the findings. Second, the retrospective study design made it impossible for researchers to control the patient's clinical variables directly. Finally, manual ROI placement still has the potential for subjectivity bias, even though its reliability has been validated through ICC testing.

CONCLUSION

This study showed that ADC values in normal adult brains showed significant regional variation between anatomical structures. There was a statistically significant difference in ADC values between grey matter and white matter networks ($p = 0.002$), where the value of grey matter was consistently higher than that of white matter in all study subjects. On the other hand, the age factor did not show a significant influence on the fluctuation in ADC values in the age range of the adult sample studied. Technically, the use of RESOLVE DWI sequences has been proven to produce highly reliable measurements with a high level of consistency. Therefore, the regional distribution map of ADC values obtained in this study can be used as a baseline to support the quantitative interpretation of MRI diffusion imaging in clinical radiology practice. Based on the research findings, several recommendations are proposed. For radiology practitioners, it is recommended to use the regional ADC value distribution map from this study as a normative baseline in interpreting diffusion-weighted imaging for patients with suspected

stroke, brain tumors, demyelinating diseases, or neurodegenerative disorders, paying attention to normal variation across brain regions to avoid misdiagnosis. For MRI technologists and medical physicists, it is recommended to adopt the RESOLVE DWI sequence as a standard protocol for brain MRI examinations, especially in artifact-prone areas like the posterior fossa and cranial base, with proper optimization of sequence parameters and ROI placement techniques to ensure measurement accuracy. For hospital radiology installations, standardized protocols for quantitative ADC measurements based on this study's reference values should be developed, alongside regular calibration and quality assurance programs for MRI scanners. For future researchers, it is recommended to expand sample sizes, conduct multicenter and longitudinal studies, investigate ADC changes in various pathological conditions, compare RESOLVE DWI with conventional DWI sequences, and explore advanced diffusion models such as diffusion kurtosis imaging or intravoxel incoherent motion (IVIM).

REFERENCE

Ahn, H. S., Kim, S. H., Kim, J. Y., Hong, M. J., & Lee, H. S. (2024). Accelerating acquisition of readout-segmented echo planar imaging (rs-EPI) with a simultaneous multislice (SMS) technique for diffusion-weighted (DW) breast MRI: Evaluation of image quality factors. European Journal of Radiology, 170(January 2023), 111251. https://doi.org/10.1016/j.ejrad.2023.111251

Calixto, C., MacHado-Rivas, F., Cortes-Albornoz, M. C., Karimi, D., Velasco-Annis, C., Afacan, O., Warfield, S. K., Gholipour, A., & Jaimes, C. (2024). Characterizing microstructural development in the fetal brain using diffusion MRI from 23 to 36 weeks of gestation. Cerebral Cortex, 34(1), 1–10. https://doi.org/10.1093/cercor/bhad409

Caravan, I., Ciortea, C. A., Contis, A., & Lebovici, A. (2018). Diagnostic value of apparent diffusion coefficient in differentiating between high-grade gliomas and brain metastases. Radiological Proceedings, 59(5), 599–605. https://doi.org/10.1177/0284185117727787

Chandra Sekhar, P., Rangasami, R., Andrew, C., & Natarajan, P. (2024). Measurement of apparent diffusion coefficient (ADC) in fetal organs and placenta using 3 Tesla magnetic resonance imaging (MRI) across gestational ages. Scientific Reports, 14(1), 1–11. https://doi.org/10.1038/s41598-024-73902-x

Di Trani, M. G., Manganaro, L., Antonelli, A., Guerreri, M., De Feo, R., Catalano, C., & Capuani, S. (2019). Apparent diffusion coefficient assessment of brain development in normal fetuses and ventriculomegaly. Frontiers in Physics, 7(OCT), 1–9. https://doi.org/10.3389/fphy.2019.00160

Ghaderi, S., Mohammadi, S., & Fatehi, F. (2025). A systematic review of diffusion microstructure imaging (DMI): Current and future applications in neurology research. Brain Disorders, 19. https://doi.org/10.1016/j.dscb.2025.100238

Grech-Sollars, M., Hales, P. W., Miyazaki, K., Raschke, F., Rodriguez, D., Wilson, M., Gill, S. K., Banks, T., Saunders, D. E., Clayden, J. D., Gwilliam, M. N., Barrick, T. R., Morgan, P. S., Davies, N. P., Rossiter, J., Auer, D. P., Grundy, R., Leach, M. O., Howe, F. A., ... Clark, C. A. (2015). Multi-centre reproducibility of diffusion MRI parameters for clinical sequences in the brain. NMR in Biomedicine, 28(4), 468–485. https://doi.org/10.1002/nbm.3269

Helenius, J., Soinne, L., Perkiö, J., Salonen, O., Kangasmäki, A., Kaste, M., Carano, R. A. D., Aronen, H. J., & Tatlisumak, T. (2002). Diffusion-weighted MR imaging in normal human brains in various age groups. American Journal of Neuroradiology, 23(2), 194–199.

Johansson, J., Lagerstrand, K., Björkman-Burtscher, I. M., Laesser, M., Hebelka, H., & Maier, S. E. (2024). Normal Brain and Brain Tumor ADC: Changes Resulting From Variation of Diffusion Time and/or Echo Time in Pulsed-Gradient Spin Echo Diffusion Imaging.

Investigative Radiology, 59(10), 727–736. https://doi.org/10.1097/RLI.0000000000001081

Lopez-Mejia, M., & Roldan-Valadez, E. (2016). Comparisons of Apparent Diffusion Coefficient Values in Penumbra, Infarct, and Normal Brain Regions in Acute Ischemic Stroke: Confirmatory Data Using Bootstrap Confidence Intervals, Analysis of Variance, and Analysis of Means. Journal of Stroke and Cerebrovascular Diseases, 25(3), 515–522. https://doi.org/10.1016/j.jstrokecerebrovasdis.2015.10.033

Luo, Y., Zhang, S., Tan, W., Lin, G., Zhuang, Y., & Zeng, H. (2022). The Diagnostic Efficiency of Quantitative Diffusion Weighted Imaging in Differentiating Medulloblastoma from Posterior Fossa Tumors: A Systematic Review and Meta-Analysis. Diagnostics, 12(11). https://doi.org/10.3390/diagnostics12112796

Martinez-Heras, E., Grussu, F., Prados, F., Solana, E., & Llufriu, S. (2021). Diffusion-Weighted Imaging: Recent Advances and Applications. Seminars in Ultrasound, CT and MRI, 42(5), 490–506. https://doi.org/10.1053/j.sult.2021.07.006

Marupudi, N. I., Altinok, D., Goncalves, L., Ham, S. D., & Sood, S. (2016). Apparent diffusion coefficient mapping in medulloblastoma predicts non-infiltrative surgical planes. Child's Nervous System, 32(11), 2183–2187. https://doi.org/10.1007/s00381-016-3168-1

Meijerink, L., van Ooijen, I., Terstappen, F., Alderliesten, T., Nievelstein, R. A. J., Lammertink, F., Benders, M., & Bekker, M. (2025). Fetal MRI study of brain differences in early-onset fetal growth restriction versus healthy controls at 30 weeks of gestation. European Journal of Obstetrics and Gynecology and Reproductive Biology: X, 27(June), 100417. https://doi.org/10.1016/j.eurox.2025.100417

Merhemic, Z., Imsirovic, B., Bilalovic, N., Stojanov, D., Boban, J., & Thurnher, M. M. (2018). Apparent diffusion coefficient reproducibility in brain tumors measured on 1.5 and 3 T clinical scanners: A pilot study. European Journal of Radiology, 108(May), 249–253. https://doi.org/10.1016/j.ejrad.2018.10.010

Mishra P, Pandey C, S. U. (2019). Descriptive Statistics and Normality Tests for Statistical Data. Annals of Cardiac Anesthesia. https://doi.org/10.4103/aca.ACA_157_18

Moradi, B., Nezhad, Z. A., Saadat, N. S., Shirazi, M., Borhani, A., & Kazemi, M. A. (2020). Apparent diffusion coefficient of different areas of brain in foetuses with intrauterine growth restriction. Polish Journal of Radiology, 85(1), e301–e308. https://doi.org/10.5114/pjr.2020.96950

Okuchi, S., Fushimi, Y., Yoshida, K., Nakajima, S., Sakata, A., Hinoda, T., Otani, S., Sagawa, H., Zhou, K., Yamao, Y., Okawa, M., & Nakamoto, Y. (2022). Comparison of TGSE-BLADE DWI, RESOLVE DWI, and SS-EPI DWI in healthy volunteers and patients after cerebral aneurysm clipping. Scientific Reports, 12(1), 1–9. https://doi.org/10.1038/s41598-022-22760-6

Osawa, T., Ohno, N., Mase, M., Miyati, T., Omasa, R., Ishida, S., Kan, H., Arai, N., Kasai, H., Shibamoto, Y., Kobayashi, S., & Gabata, T. (2021). Changes in Apparent Diffusion Coefficient (ADC) during Cardiac Cycle of the Brain in Idiopathic Normal Pressure Hydrocephalus Before and After Cerebrospinal Fluid Drainage. Journal of Magnetic Resonance Imaging, 53(4), 1200–1207. https://doi.org/10.1002/jmri.27412

Palombo, M., Bodini, B., Grussu, F., Le Bihan, D., Nilsson, M., Perez-Lopez, R., Oei, E. H. G., Schoots, I. G., Smits, M., & Jelescu, I. O. (2025). ESR Essentials: diffusion-weighted MRI—practice recommendations by the European Society for Magnetic Resonance in Medicine and Biology. European Radiology. https://doi.org/10.1007/s00330-025-12033-x

Pehlivan, U. A., Aktekin, E. H., Yalcin, C., Hasbay, B., Gunesli, A., & Alkan, O. (2024). Diagnostic Utility of Diffusion-Weighted Imaging in Distinguishing Common Pediatric Posterior Fossa Tumors: A Single Center Retrospective Study. Turkish Archives of Pediatrics, 59(6), 560–566. https://doi.org/10.5152/TurkArchPediatr.2024.24154

Saltarelli, G., Di Cerbo, G., Innocenzi, A., De Felici, C., Splendiani, A., & Di Cesare, E. (2025).

Quantitative MRI in Neuroimaging: A Review of Techniques, Biomarkers, and Emerging Clinical Applications. Brain Sciences, 15(10). https://doi.org/10.3390/brainsci15101088

Sotardi, S., Gollub, R. L., Bates, S. V., Weiss, R., Murphy, S. N., Grant, P. E., & Ou, Y. (2021). Voxelwise and Regional Brain Apparent Diffusion Coefficient Changes on MRI from Birth to 6 Years of Age. Radiology, 298(2), 415–424. https://doi.org/10.1148/RADIOL.2020202279

Spencer, A. P. C., Nguyen-Duc, J., de Riedmatten, I., Szczepankiewicz, F., & Jelescu, I. O. (2025). Mapping grey and white matter activity in the human brain with isotropic ADC-fMRI. Nature Communications , 16(1). https://doi.org/10.1038/s41467-025-60357-5

Taoka, T., Ito, R., Nakamichi, R., Nakane, T., Sakai, M., Ichikawa, K., Kawai, H., & Naganawa, S. (2022). Diffusion-weighted image analysis along the perivascular space (DWI–ALPS) for evaluating interstitial fluid status: age dependence in normal subjects. Japanese Journal of Radiology, 40(9), 894–902. https://doi.org/10.1007/s11604-022-01275-0

Widiatmoko, M. E., Tarigan, A., & Husna, M. (2024). Evaluation of MRI Brain Examination with Clinical Vertigo at dr. Drs. M. Hatta Bukittinggi Brain Hospital. Journal of Diagnostic Imaging, 10, 51–55. http://ejournal.poltekkes-smg.ac.id/ojs/index.php/jimed/index

Zhou, F., Li, Q., Zhang, X., Ma, H., Zhang, G., Du, S., Zhang, L., Benkert, T., & Zhang, Z. (2022). Reproducibility and feasibility of optic nerve diffusion MRI techniques: single-shot echo-planar imaging (EPI), readout-segmented EPI, and reduced field-of-view diffusion-weighted imaging. BMC Medical Imaging, 22(1). https://doi.org/10.1186/s12880-022-00814-5